Optical properties of different polymer thin films containing *in situ* synthesized Ag and Au nanoparticles

Rafael Abargues,*[a] Kamal Abderrafi,[a] E. Pedrueza,[a] Rachid Gradess,[b] J. Marqués-Hueso,[a] Jose Luis Valdés[a] and Juan Martínez-Pastor[a]

Received (in Montpellier, France) 7th January 2009, Accepted 21st April 2009
First published as an Advance Article on the web 2nd June 2009
DOI: 10.1039/b900185a

Here we report on the *in situ* synthesis of Ag and Au nanoparticles inside several polymer matrixes by solid-state chemical reduction of a metallic salt. Poly(ethyleneimine) (PEI), poly(hydroxyethyl methacrylate) (PHEMA), poly(vinylpyrrolidone) (PVP), novolak, poly(4-vinylphenol) (P4VP), poly(4-vinylphenol)-*co*-(methyl methacrylate) (P4VP-*co*-MMA) and poly(styrene-*co*-allyl alcohol) (PS-*co*-AA) were able to reduce Ag(I) and Au(III) to the corresponding nanoparticles during the baking process. The nanoparticle diameters of Ag and Au were found to range from 2 to 25 nm. TEM also indicated a uniform distribution of nanoparticles embedded in the thin film. This approach is suitable for controlling the size of the nanoparticles and its homogeneous distribution in the polymer matrix.

Introduction

Hybrid nanocomposites are multicomponent materials based on nanosized inorganic compounds embedded in organic polymer matrices. These materials represent an adequate solution to many present and future technological demands, because they combine the novel properties of semiconductor, metallic and magnetic nanoparticles (*e.g.*, quantum confinement, surface plasmon resonance, super-paramagnetism, respectively) with the unique properties of polymers (mechanical properties, thin film processing, conductive/dielectric properties, low cost...). Such nanoparticle–polymer composite materials are generating interest in many fields, such as optoelectronics and photonics, because of the absorption or emission properties of metallic and semiconductor nanoparticles hosted in the nanocomposite.[1–5] It is of special interest to use polymers with patternable properties since this is the first step in fabricating photonic nanostructures and more complex devices.[6–8]

Surface plasmons are collective excitations of the free electrons at the interface between a metallic structure and a dielectric. Noble metals such as Ag, Au and Cu exhibit a resonant effect at visible wavelengths. This is of great importance because plasmon excitation will then be accessible by standard optical sources and methods. At the plasmon resonance frequency, the incident electromagnetic field is locally amplified by several orders of magnitude at the metal surface of a nanoparticle. This field enhancement is responsible for the hosting of extraordinary optical phenomena exhibited by metal nanostructures, such as resonance light scattering, surface-enhanced Raman scattering[9] and superlensing.[10]

One interesting aspect of nanotechnology concerns the formation of nanoparticles on a solid support such as a thin film, given its potential for new devices involving photonics and plasmonics.[8] Two different approaches may be used to obtain metal–polymer nanocomposite films: *ex situ* and *in situ* methods. In the *ex situ* approach, the synthesis of nanoparticles is carried out by wet chemical routes and then dispersed into a polymer solution, which is finally spin coated to form a thin film.[11] However, it is difficult to disperse silver nanoparticles homogeneously into a polymer matrix by this method, because of their easy agglomeration, especially when high nanoparticle concentrations are required. In the *in situ* approach (Scheme 1), metal nanoparticles are generated inside a polymer matrix by a solid-state chemical reduction of a metallic precursor present in the polymer thin film.[6–8,12,13] This latter approach is more suitable for controlling the nanoparticle size and distribution in the polymer matrix and has the advantage of simplicity.

Up to now, only a few polymers such as PVA[6–8,12,15] and PVP[16–18] have been reported to reduce Ag(I) and Au(III) *in situ*. Here we report the synthesis of Ag and Au nanoparticles

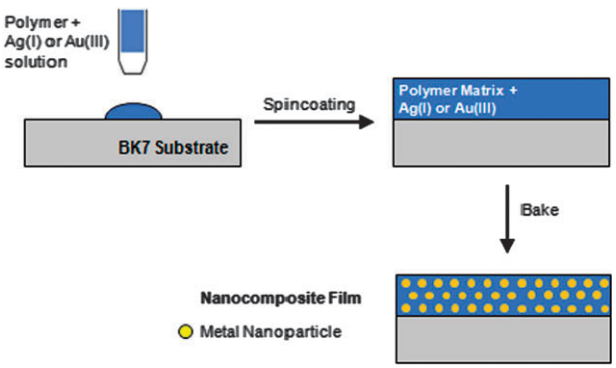

Scheme 1 Schematic diagrams of the principle of the *in situ* approach for nanocomposite film formation.

[a] *Material Science Institute, University of Valencia, P.O. Box 22085, E-46071 Valencia, Spain. E-mail: Rafael.Abargues@uv.es; Fax: +34 963543633; Tel: +34 963543622*
[b] *Department of Physics, Faculty of Sciences and Techniques, B.P. 146, 20800 Mohammedia, Morocco*

inside different polymer matrices by the solid-state chemical reduction of the metallic salt by means of a polymer. Several polymers such as poly(ethyleneimine) (PEI), poly(hydroxy ethyl methacrylate) (PHEMA), poly(vinyl pyrrolidone) (PVP), novolak, poly(4-vinylphenol) (P4VP), poly(4-vinylphenol)-*co*-(methyl methacrylate) (P4VP-*co*-MMA) and poly(styrene-*co*-allyl alcohol) (PS-*co*-AA) are considered ideal candidates as host polymers since they combine good processing capabilities (high solubility in many solvents) and excellent film-forming characteristics. Furthermore, these polymers possess certain functional groups able to produce the *in situ* reduction of Ag(I) and Au(III) salts to the corresponding nanoparticle during the baking step of the spin-coated films in a one-step procedure (Scheme 1), which is the main scope of the paper. Our results are important for the future fabrication of materials exhibiting plasmon resonance together with lithographic properties and other possible properties of interest.

Experimental

Reagents and materials

Hyperbranched poly(ethyleneimine) (PEI) (MW 25 000), poly(4-vinylphenol) (P4VP) (MW 20 000), poly(4-vinylphenol-*co*-methyl methacrylate) (P4VP-*co*-MMA), poly(2-hydroxyethyl methacrylate) (PHEMA) (MW 1 000 000), poly(styrene-*co*-allyl alcohol) (PS-*co*-AA) (MW 2200), poly(vinylpyrrolidone) (PVP) (MW 10 000), $AgNO_3$ and $KAuCl_4$ were purchased from Aldrich. Novolak formulation was purchased from a resist vendor.

Nanocomposite preparation

The polymer formulation consisted of a solution of 4 wt% of the corresponding polymer. Poly(ethyleneimine) (PEI), poly(4-vinylphenol) (P4VP), poly(4-vinylphenol-*co*-methyl methacrylate) (P4VP-*co*-MMA) and poly(styrene-*co*-allyl alcohol) (PS-*co*-AA) were dissolved in cyclohexanone, poly(2-hydroxyethyl methacrylate) (PHEMA) in ethyl-(*S*)-lactate and poly(vinylpyrrolidone) (PVP) in ethanol. Novolak formulation consisted of 10 wt% novolak, 5 wt% photoacid generator (commercial product, ma-P 1205 purchased from micro resist technology GmbH) and 85 wt% MPA. This formulation was diluted with 1-methoxy 2-propylacetate for a final polymer load of 4 wt%. $KAuCl_4$ was dissolved in one of these solvents. Because of the reduced solubility of $AgNO_3$ in the solvents in which polymers are formulated, $AgNO_3$ was dissolved in EtOH. The polymer solutions were mixed with a 0.05 M solution of $AgNO_3$ or $KAuCl_4$ in a 1 : 1 ratio. The resulting solution was spin coated on BK7 and baked at 180 or 220 °C for 10 min. The spin-coating speed was adjusted between 900 and 1300 rpm for 30 s in order to obtain film thicknesses of around 130 nm.

Characterization techniques

Transmission electron microscopy (TEM) studies of the particles were carried out at an accelerating voltage of 100 kV using a JEOL 1010 microscope. TEM samples were prepared by ultrasonicating very small pieces of BK7 in acetone with the corresponding nanocomposite thin film spin coated on it. With this procedure we obtained micrometre-sized pieces of the corresponding nanocomposites in suspension in acetone. This suspension was dropped on a carbon-coated Cu grid. The thickness of the spin-coated films was measured by using a mechanical profilometer. The composite materials were characterized by UV-Vis spectroscopy to correlate their optical properties with the size and shape of nanoparticles and their particle dispersion in the polymer matrix.

Results and discussion

Several polymers such as poly(ethyleneimine) (PEI), poly(4-vinylphenol) (P4VP), poly(4-vinylphenol-*co*-methyl methacrylate) (P4VP-*co*-MMA), poly(2-hydroxyethyl methacrylate) (PHEMA), poly(styrene-*co*-allyl alcohol) (PS-*co*-AA), poly(vinylpyrrolidone) (PVP) and novolak (Scheme 2) are considered adequate host materials for the *in situ* synthesis of Ag and Au nanoparticles during the baking process to form nanocomposite thin films.

Apart from excellent solubility in many organic solvents and excellent film-forming properties, these polymers contain functional groups with reducing properties. Novolak, P4VP and P4VP-*co*-MMA have phenolic groups that are known to possess antioxidant properties.[19] As a result, they can be oxidized to the corresponding quinone. PHEMA and PS-*co*-AA contain primary alcohols that can be oxidized to carboxylic acids (R_1COOH).[14,15] Seemingly, for amine-containing polymers such as PEI, primary amines can be oxidized to cyano groups (NCR_2) and secondary amines to imines ($R_1N{=}CR_2R_3$).[20] With respect to PVP, *N*-pyrrolidone groups can be oxidized to *N*-succinimide.[21] The number of redox electrons involved in the full oxidation of these functional group polymers is listed in Table 1. Homogeneous and transparent Ag and Au nanocomposite thin films were successfully generated during the baking process after spin coating a solution containing the host polymer and the corresponding metal salt. The baking process was generally carried out at a temperature (T_B) of around 180 °C for 10 min. However, PVP-based nanocomposite films needed

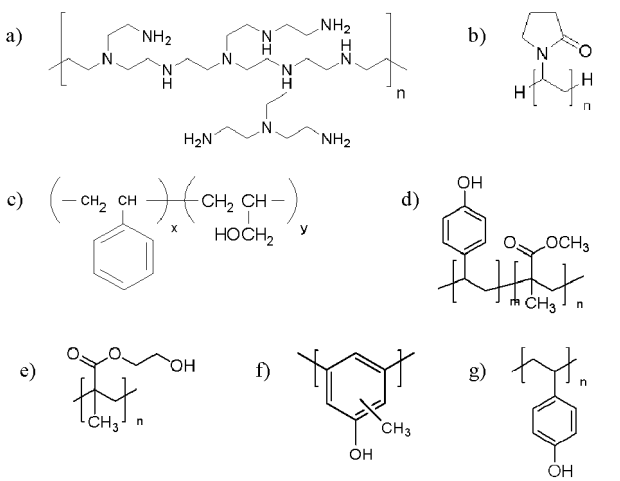

Scheme 2 Proposed host polymers. (a) Poly(ethyleneimine) (PEI), (b) poly(vinylpyrrolidone) (PVP), (c) poly(styrene-*co*-allyl alcohol) (PS-*co*-AA), (d) poly(4-vinylphenol-*co*-methyl methacrylate) (P4VP-*co*-MMA), (e) poly(2-hydroxyethyl methacrylate) (PHEMA), (f) novolak, (g) poly(4-vinylphenol) (P4VP).

Table 1 Optical properties and nanoparticle mean diameter of Au and Ag nanocomposite thin films

					Au nanocomposite				Ag nanocomposite[b]			
Polymer	T_G/°C	n_{20}[d]	Molar ratio Mon : M^{n+}	e^-_{redox}/ Mon.	λ_{LSPR}	Diameter/ nm	FT/ nm	Normal ratio Mon : Au(III)[e]	λ_{LSPR}	Diameter/ nm	FT/ nm	Normal ratio[e] Mon : Au(I)
PEI[a]	−52	1.53	1.6	28	518	4.3 ± 0.7	105	15.3	433	25.7 ± 5.2	100	45.9
PVP[b]	167–180	1.53	7.2	4	551	5.1 ± 3.2	130	9.6	413	2.6 ± 1.0	135	28.8
PHEMA[c]	102	1.51	6.2	4	549	5.9 ± 1.1	125	8.2	425	7.5 ± 1.7	120	24.6
PS_6-*co*-AA_4[a]	63	—	5.5	1.6	545	11.8 ± 4.0	124	2.9	427	8.5 ± 2.9	120	8.8
Novolak[d]	100–140	1.58	7.5	2	548	12.4 ± 3.4	125	5.0	426	7.6 ± 3.2	125	15.1
P4VP[a]	149	1.6	6.7	2	538	7.6 ± 2.5	134	4.4	430	10.1 ± 2.1	135	13.3
$P4VP_5$-*co*-MMA_5[a]	134	—	3.4	1	543	10.5 ± 3.6	119	1.2	419	4.0 ± 1.3	122	3.5

[a] Dissolved in cyclohexanone. [b] Ethanol. [c] Ethyl (*S*)-lactate. [d] Methoxypropylacetate. [e] This refers to the number of M^{n+} reduced to M(0) per monomer unit, taking into account the molar ratio Mon : M^{n+}.

T_B as high as 220 °C to generate Ag and Au nanoparticles, because the reaction takes place only above 210 °C. All these thin films were prepared from solutions with the same loading of polymer (2 wt%) and Ag(I) and Au(III) concentration (0.025 M). Because these solutions possess different viscosities due to the different chemical nature of the host polymers, the spin-coating velocity was adjusted in order to obtain the same film thickness, 130 nm (see Table 1), approximately.

The presence of Ag and Au nanoparticles in the polymer matrix was confirmed by UV-Vis spectroscopy. Fig. 1 shows the absorption spectra of the different Au and Ag nanocomposite thin films.

Typical localized surface plasmon resonances (LSPRs) of Ag and Au nanoparticles are observed at wavelengths of around 420 and 540 nm, respectively. Moreover, all these

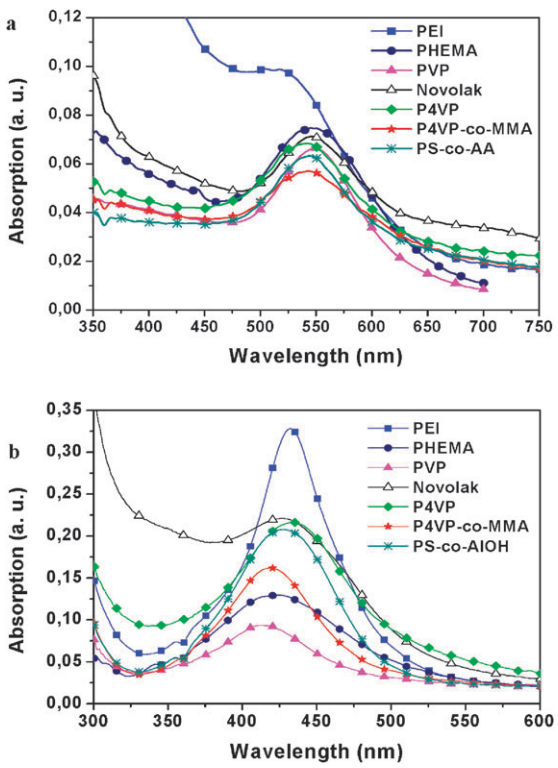

Fig. 1 UV-Vis optical properties of (a) Au and (b) Ag nanocomposite thin films.

nanocomposites showed a symmetric plasmonic absorption band. The corresponding optical properties and film thickness of the different Au and Ag nanocomposites are listed in Table 1. Among these nanocomposites, Ag–novolak and Au–PEI showed a different absorption spectrum. The Ag–novolak composite showed a shoulder around 350 nm. Novolak is a commercial photoresist that contains a photoactive compound developed for UV lithography. The shoulder exhibited at 350 nm corresponds to the absorption of this photoactive compound present in the resist formulation. The absorption of Au–PEI is related to the small size of nanoparticles generated (4.6 nm).[22]

The reduction mechanism of Ag(I) and Au(III) is illustrated in Scheme 1. In the first stage, a common solution of the host polymers, and $AgNO_3$ or $KAuCl_4$ is spin coated. In this solution, the functional groups of the host polymers (RNH_2, ROH, phenols...) complex Ag(I) and Au(III) ions. During the baking of the thin film, some of the functional groups of the host polymer chains are oxidized, and Ag(I) and Au(III) are reduced to Ag(0) and Au(0), respectively. The redox reaction takes place in the bulk polymer. Because these polymer-based films are baked above their glass transition temperature (T_G) (see Table 1), they are in their rubbery state and behave like a liquid. As a result, Ag(I) and Au(III) can diffuse with relative mobility and nanoparticles can easily nucleate, although the growth is hindered to a certain extent. As a result, Ag and Au nanoparticles are embedded in the polymer matrix to form a nanocomposite thin film. It is worth mentioning that PVP-based nanocomposites needed T_B as high as 220 °C to be well above the T_G of the polymer. Below this temperature, we observed a drastic diminution of the nanoparticle formation.

TEM was carried out to determine the corresponding shape and size of the Ag and Au nanoparticles and their distribution in the polymer matrices. Fig. 2 shows the TEM images of small pieces of nanocomposite films with Ag and Au nanoparticles embedded in the polymer. We can observe how Au and Ag nanoparticles are uniformly distributed within the polymer matrix: nanoparticles do not agglomerate and remain isolated from each other. The interparticle spacing is too high to allow plasmon coupling. This is in total agreement with the observed symmetric LSPR curves exhibited by all the nanocomposite films (see Fig. 1). With respect to the nanoparticle shape and size, Ag and Au nanocomposite thin films exhibit predominantly spherical nanoparticles with an average size of

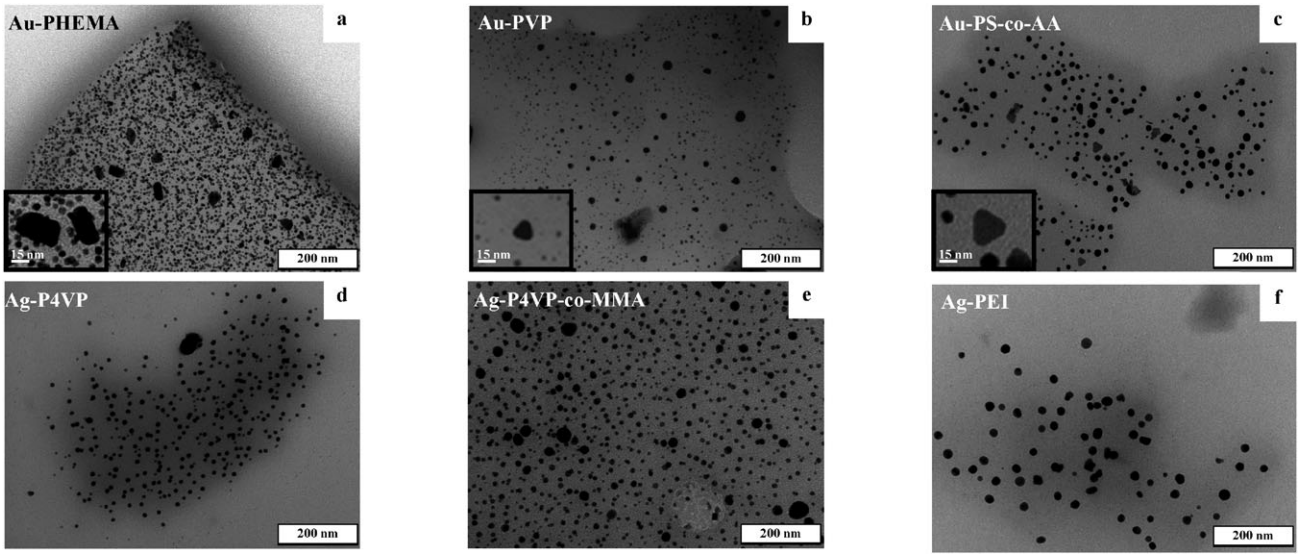

Fig. 2 TEM images of some Au and Ag nanocomposite thin films. Insets of figures a, b and c show enlarged images of some faceted nanoparticles.

4–12 nm and 2.8–26 nm, respectively. However, Au nanocomposites exhibit some triangular and faceted nanoparticles, which is indicative of their crystallinity since these shapes are typical of gold nanocrystals.[13] The actual average nanoparticle diameters of the different Au and Ag nanocomposites are also listed in Table 1. It is worth noting that the small diameter observed in these nanocomposites, especially for Au nanoparticles, is clear evidence that the growth step of nanoparticles is significantly hindered within the polymer matrices: polymers act as templates in the synthesis of nanoparticles. All these thin films were prepared from solutions with the same loading of polymer (2 wt%) and the same Ag(I) and Au(III) concentration (0.025 M). Because these solutions possess different viscosities due to the different chemical nature of the host polymers, the spin-coating conditions (rpm) were adjusted in order to obtain film thicknesses of around 130 nm (see Table 1).

As can be seen in Table 1, there are noticeable differences in the optical properties (intensity and position of the plasmonic absorption) and the nanoparticle size of the different nanocomposite thin films. The different plasmon absorptions observed in the Ag and Au nanocomposite films can be attributed to the diverse reactivity of the host polymer used. We can assume that for a given film thickness, plasmon absorption is related to the nanoparticle concentration in the polymer matrix and hence to the extent of the Au(III) and Ag(I) reduction reaction. However, it must be taken into account that the extinction coefficient of the LSPR strongly depends on the nanoparticle size and the dielectric media. Moreover, we observed different reactivities of polymers depending on the metal salt being reduced. The redox potentials of Ag(I) and Au(III) are 0.8 and 1.5 eV, respectively. Thermodynamically, Au(III) is more easily reduced to Au(0) than Ag(I) to Ag(0). When using the Au(III) salt, homopolymer-based nanocomposites (PEI, PHEMA, PVP, P4PV and novolak) exhibit higher plasmon absorption than copolymers (P4VP-*co*-MMA and PS-*co*-AA). This is attributed to the higher content of reducing groups present in the homopolymers in comparison to copolymers. Note that PS-*co*-AA and P4VP-*co*-MMA have 40 and 51 mol% of the reducing functional group, respectively. Thus, the reducing capability of the host polymers is in the following order: PEI $\gg$ PHEMA $>$ P4PV $\approx$ novolak $>$ PVP $>$ PS-*co*-AA $>$ P4VP-*co*-MMA. This is in total agreement with the monomer : Au(III) normal ratio, which is the number of Au(III) ions reduced to Au(0) per monomer unit. This is calculated taking into account the Mon : M^{n+} molar ratio and the stoichiometry of the reaction, assuming that all the redox electrons of the functional groups are involved in the reduction of Au(III) or Ag(I). Note that whereas homopolymers are in excess with respect to Au(III), the amounts of copolymers and Au(III) are almost stoichiometric, which clearly influences the kinetics of the reaction.

On the other hand, when using the Ag(I) salt this tendency is broken. The LSPR absorbance associated with Ag–PHEMA and Ag–PVP nanocomposite films was unexpectedly weak whereas that of Ag–PS-*co*-AA was surprisingly strong. The kinetics of the reduction can be different depending on the polymer used. Moreover, it is well known that Au and Ag nanoparticles have different catalytic activity and selectivity. Thus, the high LSPR absorbance achieved in PS-*co*-AA may be attributed to the fact that silver is a selective catalyst for the oxidation of styrene and other olefins.[23,24] Probably, one of the intermediates of the styrene oxidation facilitates completion of the Ag(I) reduction.

In the case of Ag–PVP, the weak LSPR may be attributed to the small mean diameter of nanoparticles (2.6 nm). Below 2 nm, nanoparticles no longer exhibit LSPR because of the low electron density in the conduction band.[22,25–27] Therefore, those nanoparticles with a diameter below 2 nm would not contribute to the plasmon absorption. In the case of PHEMA, the weak LSPR may be due to the influence of solvents in the mixture used for spin coating. Given the reduced solubility of $AgNO_3$ in the solvents in which polymers are formulated (cyclohexanone, ethyl (*S*)-lactate, and MPA), $AgNO_3$ was firstly dissolved in EtOH and then mixed with the corresponding polymer solution. It is reasonable to assume that the ethyl (*S*)-lactate–EtOH mixture may affect the extent of the Ag(I) reduction in PHEMA-based nanocomposite films.

Note that all nanocomposites were prepared under the same conditions. In any case, further dedicated work for every polymer is necessary in order to fully understand the chemistry of the formation of nanoparticles in all investigated host polymers.

The size distribution of the nanoparticles generated in the proposed polymer matrices shows different trends. Ag nanocomposite films exhibit nanoparticle average diameters from 2.6 nm for Ag–PVP to 26 nm for Ag–PEI. Au nanocomposites exhibit mean sizes from 4.6 nm for Au–PEI to 12 nm for Au–novolak. We observed a clear dependence between nanoparticle size and LSPR peak position in the case of Ag nanocomposites. This is especially significant for smaller particles. In the case of Au, we did not observe this dependence. It is known that for Au nanoparticles larger than 20 nm, the LSPR peak wavelength shifts to the red on increasing the size of the nanoparticles.[28] However, for particles smaller than 20 nm the situation becomes more complicated, with both red and blue shifts occurring. This occurs most probably due to small particle effects, including discontinuous changes to the band structure and 'spill out' of the conduction electrons.[29] The polymers used here have a refractive index between 1.51 and 1.6 for PHEMA and P4VP, respectively. However, we cannot extract from our results the real influence of the polymer refractive index on the LSPR peak position, given that nanoparticles embedded in different polymers also have different sizes.

Finally, it is worth highlighting the key role of T_B in this kind of reaction. We observed that the nanoparticle size is strongly dependent on the baking temperature used. It is well known that the formation of small particles is kinetically favored, whereas the formation of large particles is thermodynamically favored. Therefore, the dynamics of the formation of nanoparticles (nucleation and growth) are highly influenced by T_B. As a result, small nanoparticles are easily formed at lower temperatures, but these small particles have a tendency to grow into larger particles to attain a lower energy state when the reaction temperature is higher. This effect is more noticeable in Au–PVP nanocomposite films since they were baked at 220 °C. The nanoparticles in this composite exhibit an average diameter of 5.1 nm, but we observe the presence of larger nanoparticles (see Fig. 2b), which grow at the expense of the smaller ones in their neighborhood, *i.e.*, following an Ostwald ripening growth mechanism.[30] This effect is more likely to occur at higher T_B. Further work is to carry out a thorough study of the baking conditions (T_B and t_B) to optimize the formation of nanoparticles in these host polymers and to observe their possible influence on the size and shape of the resulting nanoparticles.

Conclusions

We have demonstrated that polymers with certain functional groups can *in situ* reduce Ag(I) and Au(III) salts to the corresponding nanoparticle during the baking step of the spin-coating process in a one-step procedure. Nanoparticles of different average sizes result, depending on the host polymer used. The diameter of the Ag and Au nanoparticles was found to be in the range 2.6–26 nm. Moreover, Ag and Au nanoparticles prepared by our *in situ* procedure are uniformly distributed in the polymer matrix in all cases, contrary to the *ex situ* techniques. The presence of faceted nanoparticles in Au nanocomposites is typical of gold nanocrystals. All the films exhibit LSPR absorption, thus hinting towards their application in plasmonic devices (for example, nanobiosensors). This is of special importance for PHEMA, P4VP-based and novolak polymers, since they are known to have electron beam and/or UV lithographic properties, which is the first step to fabricate devices (for example, biochips for those nanobiosensors). The present study is the base for future work devoted to fabrication of such plasmonic devices using some of the different polymers proposed here, or others having the same capabilities (functional groups able to reduce metal salts), for which the optimization of the nanoparticle production should be previously carried out.

Acknowledgements

The authors gratefully acknowledge financial support by the Generalitat Valenciana (IMPIVA-IMCITA/2007/02 and IMPIVA-IMIDIN/2008/16) and the Spanish Ministry of Science through project TEC-2005-05781-C03-03.

Notes and references

1 G. Konstantatos, I. Howard, A. Fischer, S. Hoogland, J. Clifford, E. Klem, L. Levina and E. H. Sargent, *Nature*, 2006, **442**, 180.
2 Q. Sun, Y. A. Wang, L. Li, S. Wang, D. Zhu, T. Xu, J. Ch. Yang and Y. Li, *Nat. Photonics*, 2007, **1**, 717.
3 I. Gur, N. A. Fromer, M. L. Geier and A. P. Alivisatos, *Science*, 2005, **21**(310), 462.
4 S. Sivaramakrishnan, P.-J. Chia, Y.-C. Yeo, L.-L. Chua and P. K.-H. Ho, *Nat. Mater.*, 2007, **6**, 149.
5 J. Perez-Juste, I. Pastoriza-Santos, L. M. Liz-Marzán and P. Mulvaney, *Coord. Chem. Rev.*, 2005, **249**, 1870.
6 R. Abargues, J. Marqués-Hueso, J. Canet-Ferrer, E. Pedrueza, J. L. Valdés, E. Jiménez and J. P. Martínez-Pastor, *Nanotechnology*, 2008, **19**, 355308.
7 J. Marqués-Hueso, R. Abargues, J. Canet-Ferrer, E. Pedrueza, J. L. Valdés and J. P. Martínez-Pastor, Electron beam nanopatterning of Ag and Au nanocomposite, under preparation.
8 R. Gradess, R. Abargues, A. Habbou, J. Canet-Ferrer, E. Pedrueza, A. Russell, J. L. Valdés and J. P. Martínez-Pastor, localized surface plasmon resonance sensor based on Ag–PVA nanocomposite thin films, 2009, submitted.
9 K. A. Willets and R. P. Van Duyne, *Annu. Rev. Phys. Chem.*, 2007, **58**, 267.
10 N. Fang, H. Lee, C. Sun and X. Zhang, *Science*, 2005, **308**, 534.
11 P. K. Khanna, N. Singh, S. Charan, V. V. V. S. Subbarao, R. Gokhale and U. P. Mulik, *Mater. Chem. Phys.*, 2005, **93**, 117.
12 W. Fritzche, H. Porwol, A. Wiegand, S. Bornmann and J. M. Köhler, *Nanostruct. Mater.*, 1998, **10**, 89.
13 S. Porel, S. Singh, S. S. Harsha, D. N. Rao and T. P. Radhakrishnan, *Chem. Mater.*, 2005, **17**, 9.
14 K.-S. Chou and C.-Y. Ren, *Mater. Chem. Phys.*, 2000, **64**, 241.
15 S. Clémenson, L. David and E. Espuche, *J. Polym. Sci., Part A: Polym. Chem.*, 2007, **45**, 2657.
16 R. He, X. F. Qian, J. Yin and Z. K. Zhu, *J. Mater. Chem.*, 2002, **12**, 3783.
17 M. Tsuji, M. Hashimoto, Y. Nishizawa, M. Kubokawa and T. Tsuji, *Chem.–Eur. J.*, 2005, **11**, 440.
18 T. Yamamoto, H. B. Yin, Y. J. Wada, T. Kitamura, T. Sakata, H. Mori and S. Yanagida, *Bull. Chem. Soc. Jpn.*, 2004, **77**, 757650.
19 Z. Rappoport, *The chemistry of phenols*, John Wiley & Sons, New York, 2003.
20 A. Ricci, *Amino Group Chemistry*, Wiley-VCH, Verlag, 2008.

21 M. A. Tallon, E. G. Malawer, N. I. Machnicki, P. J. Brush, C. S. Wu and J. P. Cullen, *J. Appl. Polym. Sci.*, 2007, **5**, 107.
22 V. Myroshnychenko, J. Rodríguez-Fernández, I. Pastoriza-Santos, A. M. Funston, C. Novo, P. Mulvaney, L. M. Liz-Marzán and F. J. García de Abajo, *Chem. Soc. Rev.*, 2008, **37**, 1792–1805.
23 Z. M. Hu, H. Nakai and H. Nakatsuji, *Surf. Sci.*, 1998, **401**, 371.
24 R. J. Chimentão, I. Kirm, F. Medina, X. Rodríguez, Y. Cesteros, P. Salagre, J. E. Sueiras and J. L. G. Fierro, *Appl. Surf. Sci.*, 2005, **252**, 793.
25 A. R. Graham, H. M. Dan and N. K. Andrei, *Chem. Phys. Lett.*, 2008, **460**, 230–236.
26 M. M. Maye, L. Han, N. N. Kariumi, N. K. Ly, W.-B. Chan, J. Luo and C.-J. Zhong, *Anal. Chim. Acta*, 2003, **496**, 17.
27 M. L. Rodríguez-Sánchez, M. J. Rodríguez, M. C. Blanco, J. Rivas and M. A. López-Quintela, *J. Phys. Chem. B*, 2005, **109**(3), 1183–1191.
28 S. Link and M. A. El-Sayed, *J. Phys. Chem. B*, 1999, **103**, 8410.
29 U. Kreibig and M. Vollmer, *Optical Properties of Metal Clusters*, Springer, London, 1995.
30 A. R. Roosen and W. C. Carter, *Physica A (Amsterdam)*, 1998, **261**, 232.